RSC Advances

PAPER

View Article Online
View Journal | View Issue

Cite this: *RSC Adv.*, 2017, **7**, 35330

Hierarchically structured carbon nanotube–polyaniline nanobrushes for corrosion protection over a wide pH range†

Guodong Qiu,[a] Aiping Zhu*[a] and Chaoqun Zhang *[b]

Received 9th May 2017
Accepted 7th July 2017

DOI: 10.1039/c7ra05235a

rsc.li/rsc-advances

Carbon nanotube–polyaniline brush-like nanostructures have been successfully synthesized through *in situ* oxidative polymerization of aniline on the surface of carboxylated multi-walled carbon nanotubes. The diameter of the resultant tubular nanobrushes is dependent on the mass ratio of c-MWNTs to aniline. The as-designed carbon nanotube–polyaniline nanobrushes exhibit superior electroactivity not only in acidic, but also in neutral and alkaline environments. The excellent anticorrosion performance has been achieved by incorporation of these nanobrushes into amine cured epoxy modified acrylic resin. It is found that the good barrier property of the nanobrush coating against neutral and alkaline corrosion media penetration and its predominant passivation protection against acidic medium offer anticorrosion protection for steel over a wide pH range. The novel carbon nanotube–polyaniline nanobrushes prepared using this facile route extend the application of polyaniline to a wider range of pH environments and facilitate a more environmentally friendly and economical system than traditional heavy metal coatings and their oxide coatings, in the application of anticorrosion protection of metals.

1. Introduction

Among the conducting polymers, polyaniline (PANI) has been found to be one of the most promising materials for wide applications in rechargeable batteries[1,2] electrocatalysis,[3] electrochromic devices,[4] conversion of light to electricity and corrosion resistance[5,6] due to its tunable conductivity, good environmental stability, nontoxic property and low cost.[7–9] Since Deberry first reported the protective effect of PANI on steels for long periods in sulfuric acid solution,[10] the PANI based coatings have been considered in applications for the anticorrosion protection of aluminum, iron, copper and other metals, as a replacement for traditional heavy metal coatings and their oxide coatings.[11–13]

Several mechanisms underlying the protective behavior of PANI coatings have been proposed and reported, such as physical barrier protection, passivation protection, corrosion inhibition, electric field effect, *etc.*[14,15] The passivation protection of steel by PANI has been reported to be the most efficient in which a thin oxide protective layer is formed as a result of electrochemical interaction between the polymer and metal surface. Wessling *et al.* reported that the passive iron oxide layer was formed between PANI coatings and the metal surface after immersed in 3 wt% NaCl solution, resulting in decrease of the corrosion current and increase of the corrosion potential revealed by Tafel polarization curve test.[16] Talo *et al.* found that the metal surface with PANI containing epoxy coating presented gray color after immersed in 0.6 M NaCl solution for a period of time. X-ray photoelectron spectroscopy (XPS) revealed that these color change are results of the formation of iron oxides.[17] Chen *et al.* studied the anticorrosion property of epoxy coating filled with PANI and found an obvious increase on the resistance of the coating in neutral solution during 30 day of immersion, which indicated the formation of a passivation layer between the metal surface and coating.[18] However, the occurrence of deprotonation of PANI when pH >4 greatly reduces its conductivity and electroactivity,[19,20] leading to the loss of passivation protection of PANI in basic solution. Thus, the practical application of PANI as anticorrosion coatings is limited, especially in the application of marine corrosion protection with high pH values (pH $\geq$ 7).

The use of aniline derivatives and polymer blends with acid doping mechanism is an efficient and economical way to reduce the pH dependence of redox activity of PANI. For example, Mu *et al.* investigated the copolymerization of 5-aminosalicylic acid and *p*-aminophenol with aniline by introducing pH functional groups of –COOH and –OH into PANI polymer backbone to maintain a good electroactivity in a wide pH range.[21] Advincula *et al.* showed that the electroactivity of PANI can be shifted to neutral electrolytes by doping PANI with macromolecular acids such as poly(acrylic acid) poly(vinyl sulfonate) and poly(styrene

[a]*School of Chemistry and Chemical Engineering, Yangzhou University, Yangzhou 225002, China. E-mail: apzhu@yzu.edu.cn; Tel: +86 0514 87993691*

[b]*College of Materials and Energy, South China Agricultural University, Guangzhou 510642, China. E-mail: nwpuzcq@gmail.com*

† Electronic supplementary information (ESI) available. See DOI: 10.1039/c7ra05235a

sulfonate), in which strong interactions existed between poly(anions) with polyaniline chains.[22,23] However, the electroactivity of all these PANI complexes still decayed to certain degree with increasing pH from acid to alkaline environments. The incorporation of conductive nano-fillers into polymer matrix based on charge transfer doping mechanism is another promising way to solve this problem due to their synergistic and complementary behaviors. The conductive carbon-based nanomaterials such as carbon nanotubes (CNTs)[24,25] as the dopant would be preferred due to its large specific surface area, remarkable performance in terms of mechanical, electrical, and thermal properties. Liu *et al.* used LBL self-assembly method to prepare PANI/CNTs multilayer films by alternating immersion of Au substrate into the solutions of polyaniline (PANI) and poly(aminobenzenesulfonic acid)-modified single-walled carbon nanotubes and the multilayer film has stable electrochemical activity in neutral solution.[24] Zhou *et al.* prepared PANI/CNTs nanocomposite by simply mixture of polyaniline emeraldine base (PANI) with pristine single-walled carbon nanotubes and found that the effective doping of CNTs on PANI can maintain its electroactivity with a fast electron transfer property and a high stability in the neutral and alkaline medium.[25]

In this work, hierarchically structured carbon nanotube–polyaniline nano-brushes (c–PANI) were prepared by *in situ* polymerization with carboxylated carbon nanotubes (c-MWNTs) as charge transfer doping agents. The effects of mass ratio of c-MWNTs to aniline on the morphologies and structures of the final composites were investigated. Transmission electron microscopy (TEM), Fourier transform infrared spectroscopy (FTIR), Ultraviolet-visible spectroscopy (UV-vis), and X-ray Powder Diffraction (XRD) were used to characterize the carbon nanotube–polyaniline composites. The cyclic voltammetry (CV) measurements showed that the construction of the unique nanobrush structure leads to the formation of new charge transfer doping through π–π stacking interactions and hydrogen bonding between carbon nanotubes and polyaniline, resulting in superior electroactivity not only in acidic, but also in neutral and alkaline environments. Furthermore, the mechanism by which these nanobrush-containing amine cured epoxy modified acrylic resins coatings afford corrosion protection towards carbon steel has been investigated and discussed.

2. Experimental

2.1 Materials

Carboxylated multi-walled carbon nanotubes (purity 95%, diameter 10–20 nm, length 10–30 μm) were purchased from Beijing DK nano technology Co. Ltd. Aniline, ammonium persulfate (APS), sulfuric acid and ethanol were purchased from Sinopharm Chemical Reagent Co. Ltd. Dodecyl diphenyl ether sodium sulfonate used as the anionic surfactant (2A1) was provided by DOW Co. Ltd. Epoxy modified acrylic resin, amino resin curing agent and organic phosphoric acid catalyst from Sanmu Group Co. Ltd. were used to prepare waterborne coatings.

2.2 Preparation of c–PANI nanobrushes

The c–PANI nanobrushes were prepared *via* oxidative polymerization of aniline on the surface of c-MWNTs. Briefly, 0.116, 0.233, 0.466 and 0.931 g of c-MWCNT were respectively dispersed in 80 mL distilled water, followed by the addition of 0.01 mol aniline monomer and 9.3 mg of 2A1 as dispersant. The mixture was further dispersed with the combination of stirring and ultrasonication for 1 h. Subsequently, an appropriate amount of concentrated sulfuric acid was used to adjust the pH of the solution to 1. Then, 20 mL of 0.05 mol L^{-1} H_2SO_4 aqueous solution containing 0.01 mol APS was added dropwise into the as-prepared suspension in an ice bath. The reaction was allowed with a moderate stirring at a reaction temperature of 0–5 °C for 6 h. Finally, c–PANI nanobrushes were obtained by washing with ethanol, water and 0.05 mol L^{-1} H_2SO_4 aqueous solution and drying in vacuum at 80 °C for 24 h.

2.3 Preparation of PANI and c–PANI containing epoxy modified acrylic resin coatings

PANI or c–PANI nanobrushes were dispersed into epoxy modified acrylic resin followed by the uniformly addition of the amino resin curing agent and organic phosphoric acid catalyst. A dipping method was used followed by curing at 130 °C for 0.5 h to form coating with about 30 μm of thickness on steel bars for anticorrosion analysis.

2.4 Characterization

The morphologies of PANI and the c–PANI composites were analyzed by transmission electron microscopy (TEM; Philips Tecnai12, 200 kV). X-ray diffraction (XRD) data were collected from 10° to 80° (2θ angle) from a Bruker AXS D8 ADVANCE X-ray diffractometer using Cu Kα radiation (40 kV, 40 mA). Fourier transform infrared (FTIR) spectroscopy was performed on a Bruker VECTOR 22 spectrometer using KBr sample pellets. The UV-vis spectra of 0.01 g sample in 10 mL of *N*-methyl-2-pyrrolidone (NMP) were obtained using a PERSEE TU-1901 spectrophotometer. Optical micrographs of waterborne coatings were taken by a MA-2001 optical microscope. CV tests were performed on a CHI660a electrochemical station using a three-electrode configuration in Swagelok cells. The electrolytes was 3.5% NaCl. The working electrodes were prepared by drop-casting the composite suspension (1 wt%, in methanol) on glassy carbon steel stick. The counter and reference electrodes were a platinum foil and a Ag/AgCl electrode, respectively. Electrochemical impedance spectroscopy (EIS) measurements were performed with an EcoChemie AutoLab 302N analyzer. A three-electrode cell was also used employing the coated steel as a working electrode with an exposed area of 4.7 cm^2, a platinum foil and a saturated Hg/Hg_2Cl_2 electrode as counter and reference electrodes, respectively. XPS measurements were conducted on an ESCALAB 250Xi spectrometer with an Al Kα X-ray source (1486.5 eV). For the sample of XPS analysis, the soaked coating was carefully striped away and to expose the underlying steel surfaces.

3. Results and discussion

Carbon nanotube–polyaniline brush-like nanostructures have been synthesized through *in situ* oxidative polymerization of aniline on the surface of carboxylated multi-walled carbon nanotubes as shown in Fig. 1. The interactions between PANI and nanotubes take place as a consequence of the oxidation polymerization, including π–π stacking between quinoid ring of PANI and the π-bonded surface of nanotubes, hydrogen bonding between –OH groups on the surface of nanotubes and –NH of PANI, and electrostatic interaction between $–COO^-$ groups of nanotubes and $–NH^+$ of PANI. The morphology and chemical structures of the resulting carbon nanotube bushes were characterized by TEM, FTIR, UV-vis, and XRD, respectively.

Fig. 2 shows the TEM images of c–PANI nanobrushes. The image of pristine PANI is also presented for comparison. Fig. 2a shows clearly that PANI exhibits a short-fiber morphology with serious agglomerate. It is also show that (Fig. 2b–e) a tubular layer of PANI is uniformly coated on the surface of c-MWCNT through oxidative polymerization. These composites demonstrate homogeneous nanobrush structures in which c-MWCNT serves as the conductive core and PANI as the hair brushes. The diameter of these tubular c–PANI is dependent on the mass ratio of c-MWNTs to aniline (W_r). As W_r increases from 1 : 8 to 1 : 4, the diameters of the composites decreases from 50 nm (Fig. 2b) to 20 nm (Fig. 2c). When W_r continue to increase to 1 : 2 and 1 : 1, the diameters of the composites decreases sharply but still larger than that of pure c-MWNTs. After the formation of c–PANI composites, these c-MWNTs are found to be entrapped in PANI chains leading to increase of the c–PANI size. Obviously, the PANI chains are dispersed and glued into surface of c-MWNTs, not simply mixed up or blended with c-MWNTs, resulting in less agglomerate behavior of PANI without any surfactant.[26]

Fig. 3 showed the FTIR spectra of PANI and c–PANI nanobrushes. The FTIR spectrum of PANI display the typical vibration modes with bands at 3423 cm^{-1} (N–H stretching), 1562 cm^{-1} (C=

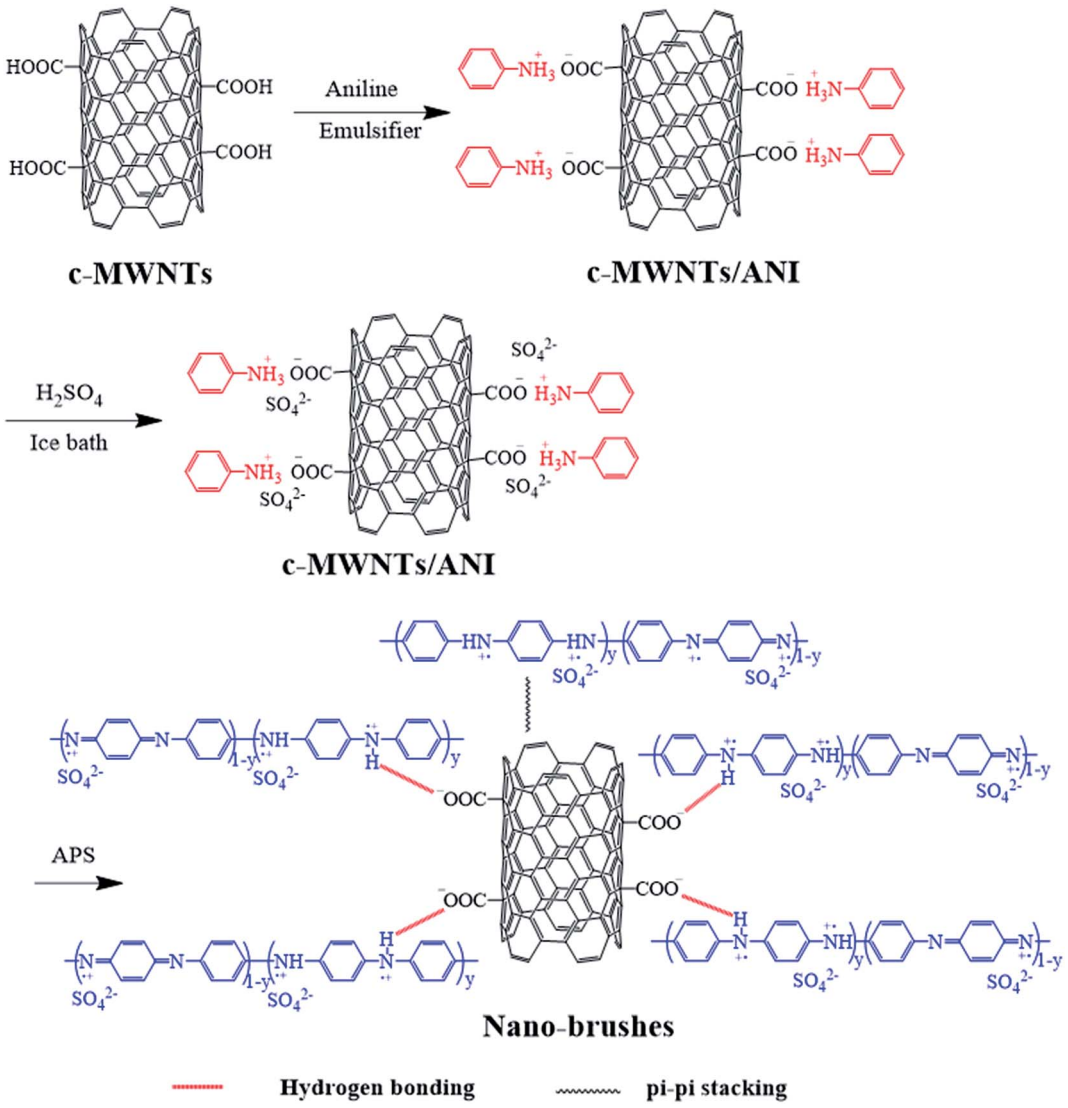

Fig. 1 The scheme of preparation of c–PANI composite.

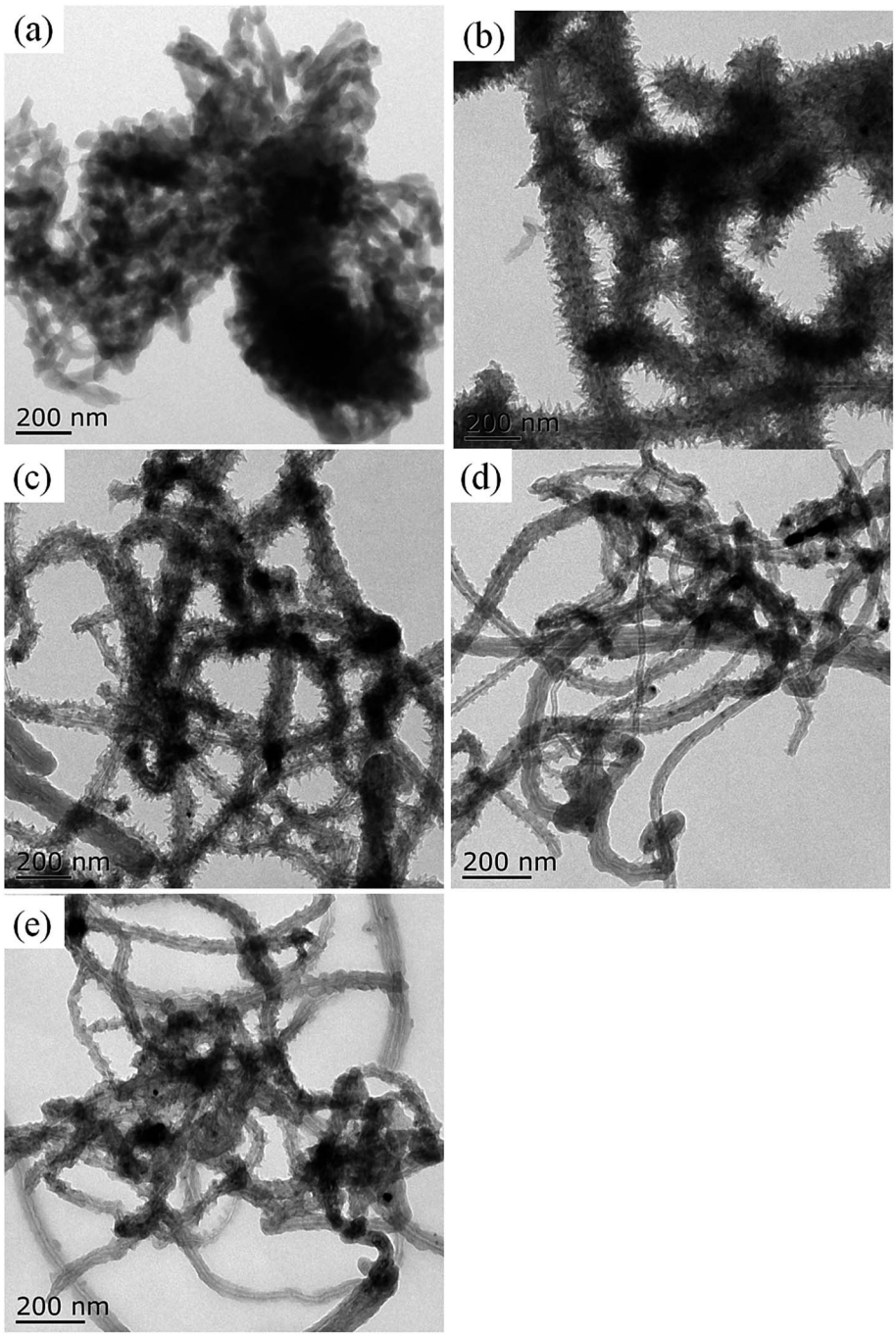

Fig. 2 TEM images of PANI (a) and c–PANI nanobrushes prepared with the W_r of (b) 1 : 8; (c) 1 : 4; (d) 1 : 2 and (e) 1 : 1.

C stretching, quinoid rings), 1476 cm^{-1} (C═C stretching, benzenoid rings), 1299 cm^{-1} (C–N stretching, quinoid rings), 1231 cm^{-1} (C–N stretching, benzenoid rings).[27] With increasing content of c-MWNTs, the peaks at 1562 cm^{-1} and 1299 cm^{-1} gradually shift to lower wave numbers (1543 cm^{-1}, 1286 cm^{-1}). In addition, a notable increase in the intensity ratio of the quinoid to benzenoid ring is observed for c–PANI nanobrushes. The quinoid peak is a measurement of the degree of delocalization of the electrons and, thus, it is a characteristic peak of electrical transport.[28] This suggests that interactions between PANI and nanotubes take place as a consequence of the oxidation polymerization as shown in Fig. 3, including π–π stacking between quinoid ring of PANI and the π-bonded surface of nanotubes, hydrogen bonding between –OH groups on the surface of nanotubes and –NH of PANI, and electrostatic interaction between $–COO^-$ groups of nanotubes and $–NH^+$ of PANI.[29] Furthermore, these interactions facilitate charge-transfer processes between the PANI and nanotubes, and thereby influence the transport properties of the composites.

The dominant features between the PANI and nanotubes is also confirmed by the UV-vis spectra of PANI and c–PANI composites (Fig. 4). The absorption peak corresponding to the

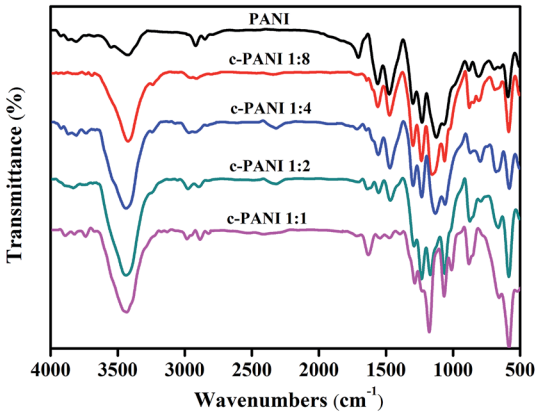

Fig. 3 FTIR spectra of PANI and c–PANI nanobrushes prepared at different W_r.

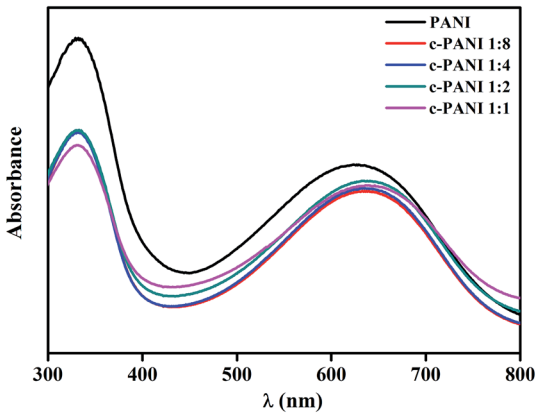

Fig. 4 UV-vis spectra of PANI and c–PANI composites prepared at different W_r.

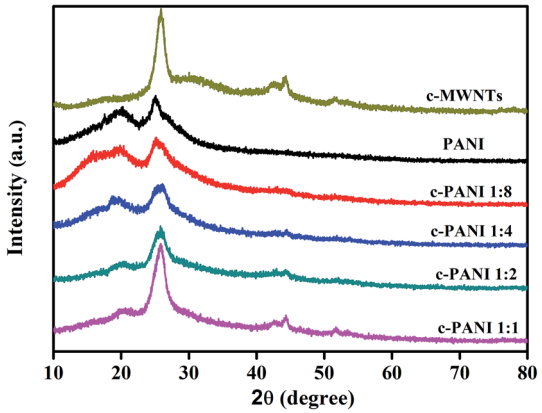

Fig. 5 XRD patterns of c-MWNTs, PANI and c–PANI composites prepared at different W_r.

transition of the exciton of the quinone shifted from 627 nm to 639 nm after the formation of composites. A similar red-shifted was also reported on PANI/graphene systems, which is ascribed by the interactions between c-MWNTs and quinoid ring in PANI.[30]

The powder XRD patterns of c-MWNTs, PANI and c–PANI composites are shown in Fig. 5. The diffraction peaks of c-MWNTs appear at $2\theta = 25.8°$ and 44.2° representing the crystal planes of (002) and (100) of graphite.[31] The crystalline peaks of pristine PANI appear at $2\theta = 15.9°$, 19.9° and 24.9°, corresponding to (011), (020) and (200) crystal planes in its emeraldine salt state, respectively.[32] The patterns of c–PANI composites possess all characteristic diffraction peaks of c-MWNTs and PANI. The intensity of conspicuous peak at $2\theta = 19.9°$, corresponding to the periodicity of the crystallographic planes that are perpendicular to the doped PANI chains,[33] decreases obviously when the W_r increases from 1 : 4 to 1 : 1. And the intensity of peak at $2\theta = 44.2°$ increases with increasing W_r from 1 : 4 to 1 : 1. This result indicates that c-MWNTs as a charge transfer dopant for PANI compete with sulfuric acid dopant, and influence the crystallinity of PANI through the π–π stacking and hydrogen bonding interactions between c-MWNTs and PANI.

To further elucidate the charge transfer effect of c-MWNTs on the electroactivity of PANI, the electrochemical activities of PANI and c–PANI composites were studied by CV measurements in 3.5 wt% NaCl with pH of 1, 7 and 9 at 25 °C, respectively. As shown in Fig. 6, each curve exhibits a similar shape with two pairs of redox at pH of 1. The redox peaks for PANI locate at around 0.10/0.22 V and 0.61/0.68 V as shown in Fig. 6a, which could be attributed to the redox transitions between leucoemeraldine and emeraldine, and the faradaic transformation of emeraldine to pernigraniline,[34] respectively. In the case of c–PANI composites, the cathodic redox peaks shift negatively while the anodic redox peaks shifted positively with the increase content of c-MWNTs. The c–PANI composites with W_r of 1 : 8, 1 : 4 and 1 : 2 demonstrate enhanced peak intensities, indicating high electroactivity over the pristine PANI in acid medium. The decreased peak intensity of c–PANI composites with W_r of 1 : 1 may result from less PANI coated heterogeneous on the surface of MWCNT as evidenced by the TEM images discussed above. As reported, the electroactivity of the pristine PANI is relevant to its doping lever.[25] Obviously, c-MWNTs dope PANI directly through the charge-transfer interactions, leading to the variation of electroactivities of c–PANI composites.[35]

Generally, the electrochemical activity of the pristine PANI loses completely at pH ≥7 with disappearance of the redox peaks due to the deprotonation of PANI in neutral and base medium[20,21] as shown in Fig. 6b and c. However, the c–PANI nanobrushes demonstrate a different phenomenon with the pristine PANI when pH ≥7. In neutral medium, the c–PANI composites with W_r of 1 : 8, 1 : 4 and 1 : 2 still have two obvious redox peaks. In alkaline medium, the c–PANI composites with W_r of 1 : 8 and 1 : 4 also demonstrate two pairs of redox peaks. All these results indicated that the c–PANI composites in this study demonstrate much higher electrochemical activity than CNT/PANI systems reported before in which only one pair of irregular redox peaks appeared for electrochemical response at neutral electrolytes.[36,37] The superior electroactivity of the c–PANI composites in high pH environments is resulted from the novel nanobrush morphology with c-MWNTs encapsulated by PANI perfectly especially for the c–PANI composites with W_r of

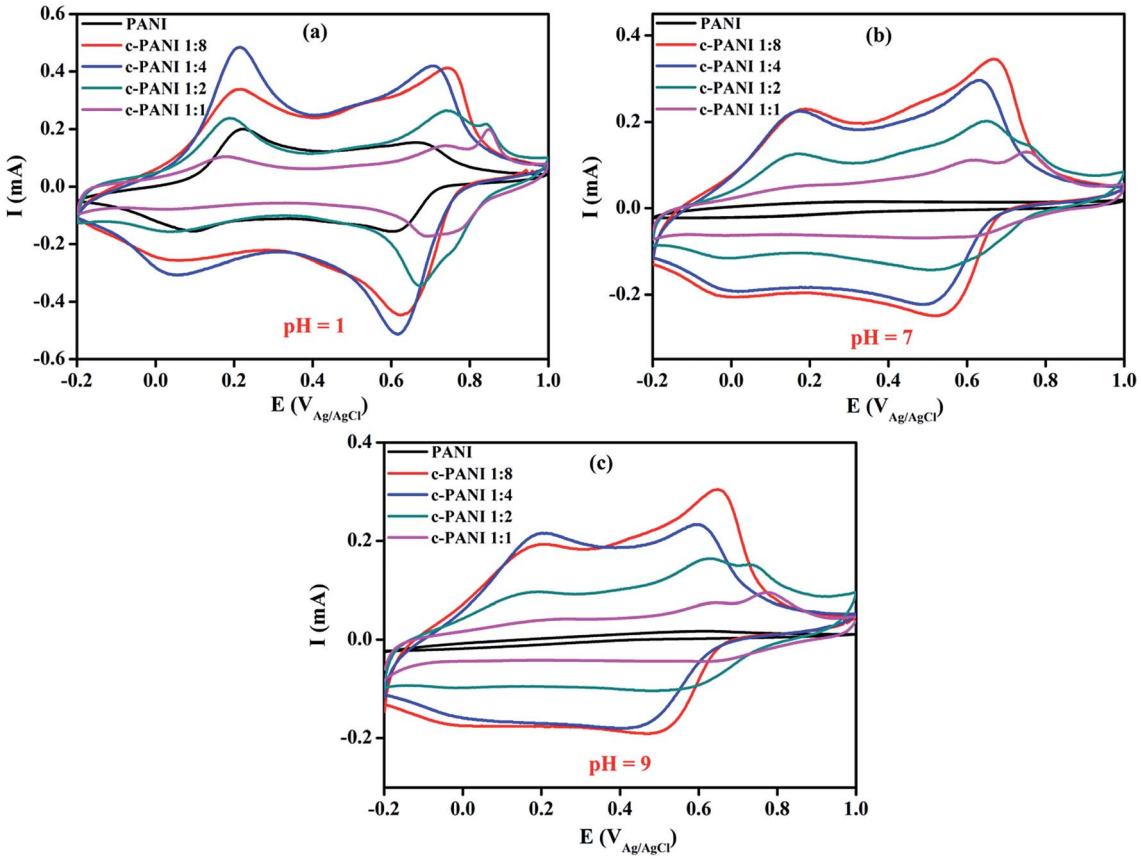

Fig. 6 Cyclic voltammograms of PANI and c–PANI composites (a) in the electrolyte of pH 1; (b) in the electrolyte of pH 7; (c) in the electrolyte of pH 9.

1 : 8 and 1 : 4. The strong interface interaction through the π–π stacking between PANI and c-MWNTs facilitate the electron delocalization, which forms doped PANI mainly by charge transfer in the process of redox.[25] Unlike protonic acid doping, charge transfer doping is almost insusceptible to pH. In this specific system, both charge transfer doping and protonic acid doping exist in present c–PANI composite system. As a result, the redox peaks of the composite with W_r of 1 : 1 decrease compared with PANI, and the redox peaks of all the composites still become weak with increasing pH to high value.

To investigate the effect of these novel nanobrushes on the anticorrosion performance, PANI and c–PANI nanobrushes with W_r of 1 : 8 were selected to fill into amine cured epoxy modified acrylic acid resin for a waterborne PANI-based coating on carbon steel. The optical micrographs of composites with different c–PANI contents are shown in Fig. 7. Obviously, c–PANI dispersed well in resin matrix with little aggregation compared (Fig. 7b–d) with that of PANI (Fig. 7a). This result indicates that the composites with nanobrush morphology of c-MWNTs encapsulated with PANI can prevent both the aggregation of c-MWNTs and PANI nanoparticles. c–PANI/epoxy coating with 3 wt% loading was used for the following electrochemical protection investigation.

The electrochemical behavior of the c–PANI/epoxy coatings was investigated by EIS in the mediums with different pH as shown in Fig. 8. The test of PANI/epoxy coatings are also conducted to allow a comparison. One of the electrochemical parameters to evaluate the anticorrosion properties of the coatings was the impedance modulus ($|Z|_{0.1\ Hz}$) at the lowest frequency (0.1 Hz).[38] At the initial immersion, the $|Z|_{0.1\ Hz}$ reflected the pore resistance of the coating resulting from water and electrolyte penetration.[18] The $|Z|_{0.1\ Hz}$ of c–PANI coating is $3.32 \times 10^8\ \Omega\ cm^2$, $2.04 \times 10^8\ \Omega\ cm^2$ and $1.81 \times 10^8\ \Omega\ cm^2$ after soaking in acidic, neutral and alkaline medium for 1 day while the $|Z|_{0.1\ Hz}$ of PANI coating is $4.45 \times 10^7\ \Omega\ cm^2$, $3.85 \times 10^7\ \Omega\ cm^2$ and $3.32 \times 10^7\ \Omega\ cm^2$ respectively. Obviously at the initial immersion, the $|Z|_{0.1\ Hz}$ of c–PANI coating is almost 10 times over that of PANI coating, which confirmed the improved better barrier property of c–PANI coating than pure PANI coating.

In acidic medium, the $|Z|_{0.1\ Hz}$ of PANI coating decreased with prolonging soaking days obviously. Its $|Z|_{0.1\ Hz}$ decreased to $1.03 \times 10^6\ \Omega\ cm^2$ after 16 days of soaking, indicating failed protection of the coating. In contrast, the $|Z|_{0.1\ Hz}$ of c–PANI coating in the same solution increased slightly to $3.5 \times 10^8\ \Omega\ cm^2$ after 4 days of soaking, and decreased to $6.83 \times 10^6\ \Omega\ cm^2$ at 16 days. The presence of an initial increase in the $|Z|_{0.1\ Hz}$ value reflected significant passivation of steel occurred in the acidic medium.

In neutral medium, the $|Z|_{0.1\ Hz}$ of PANI coating decreased with the increase of soaking time, and to $6.88 \times 10^6\ \Omega\ cm^2$ at 16

days; in alkaline medium, the $|Z|_{0.1\ Hz}$ of PANI coating decreased to $9.02 \times 10^5\ \Omega\ cm^2$ (low than $10^6\ \Omega\ cm^2$), meaning losing the ability of corrosion protection. Although the $|Z|_{0.1\ Hz}$ of c–PANI coating also decreased with increasing soaking time in neutral and alkaline medium, its $|Z|_{0.1\ Hz}$ still maintains $7.21 \times 10^7\ \Omega\ cm^2$ and $8.72 \times 10^7\ \Omega\ cm^2$ after 16 days of soaking in neutral and alkaline medium respectively.

It is known that electrolyte penetrating power is strong in acidic or alkaline medium than in neutral medium. Thus the $|Z|_{0.1\ Hz}$ will unavoidable decrease greatly as comparison in neutral medium. Generally, the relative better anticorrosion performance of PANI coating in acidic medium than that in alkaline medium should owe to the redox activity of PANI. Chen *et al.* have reported that the redox property of PANI, in which PANI–Emeraldine Salt (PANI–ES) could be reduced to PANI–Leucosalt (PANI–LS) through the oxidation of Fe to Fe^{2+} or Fe^{3+}, and be reoxidized to PANI–ES in corrosive environment, could enhance the anticorrosion performance of coatings.[17] In alkaline medium, PANI coating failed to provide corrosion protection for steel due to loss of redox activity of PANI as discussed above. However, c–PANI coating has anticorrosion performance not only in acid or neutral but also in alkaline medium. The possible explanation of the present results is the evident electroactivity of c–PANI enhanced in the medium of pH 7 and pH 9, which promote the electrochemical corrosion protection of c–PANI coating.

To further understand the corrosion protection mechanism of c–PANI, Bode plots of waterborne c–PANI coating soaked in medium with different pH by prolonging the soaking time to 35 days is shown in Fig. 9. In neutral and alkaline medium, the $|Z|_{0.1\ Hz}$ of c–PANI coating decreases gradually with prolonging the soaking days. But $|Z|_{0.1\ Hz}$ still remains $1.67 \times 10^7\ \Omega\ cm^2$ and $1.07 \times 10^7\ \Omega\ cm^2$ after 35 days of soaking in neutral and alkaline medium, respectively, demonstrating excellent corrosion protection behavior. This should be caused by the redox activity of c–PANI in pH 7 and 9 and the barrier property brought by the uniformly dispersion of c–PANI with nanobrush morphology.

However, in acidic medium, the exciting result of c–PANI coating appears. The $|Z|_{0.1\ Hz}$ decrease sharply from $3.32 \times 10^8\ \Omega\ cm^2$ with soaking 1 day to $1.64 \times 10^6\ \Omega\ cm^2$ for soaking 20 days, which may be due to the partly loss of adhesion of the coating to the metal in acidic medium. Afterward the $|Z|_{0.1\ Hz}$ increased to $7.59 \times 10^7\ \Omega\ cm^2$ after 30 days of soaking and decreased again to $5.39 \times 10^6\ \Omega\ cm^2$ after 35 days of soaking. This variation of $|Z|_{0.1\ Hz}$ should corresponds to passivation effect of c–PANI on metal surface, in which the electroactivity property of c–PANI could make it participate in corrosion reaction and contribute to the formation of a passivation layer on the metal surface.[39]

Tafel plots for PANI and c–PANI coating electrodes measured in pH 3, pH 7, and pH 9 in 3.5% NaCl aqueous solution after immersion for 16 days were shown in Fig. 10. Electrochemical corrosion measurements of coatings with PANI and c–PANI as fillers in different solution were recorded in Table 1, respectively. Generally, a higher E_{corr} and a lower I_{corr} indicate better

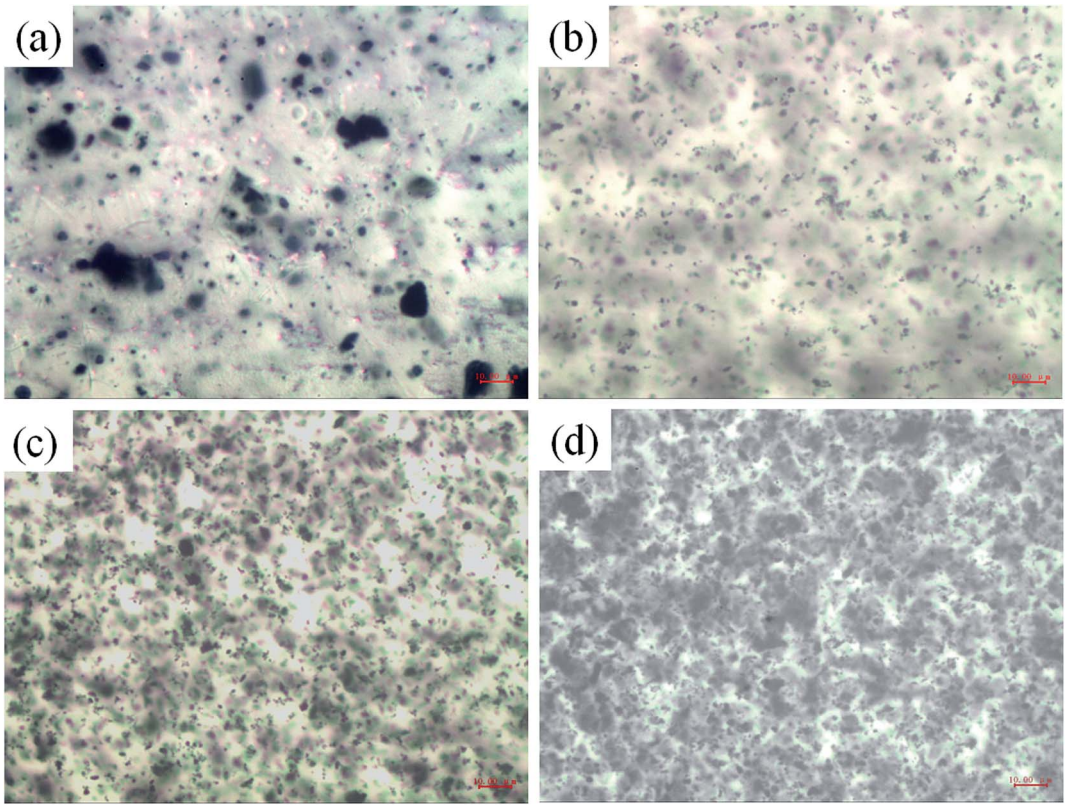

Fig. 7 Optical micrographs of waterborne amine cured epoxy modified acrylic acid resin with PANI loading of (a) 3 wt% and c–PANI loading of (b) 1 wt%; (c) 3 wt%; (d) 5 wt%.

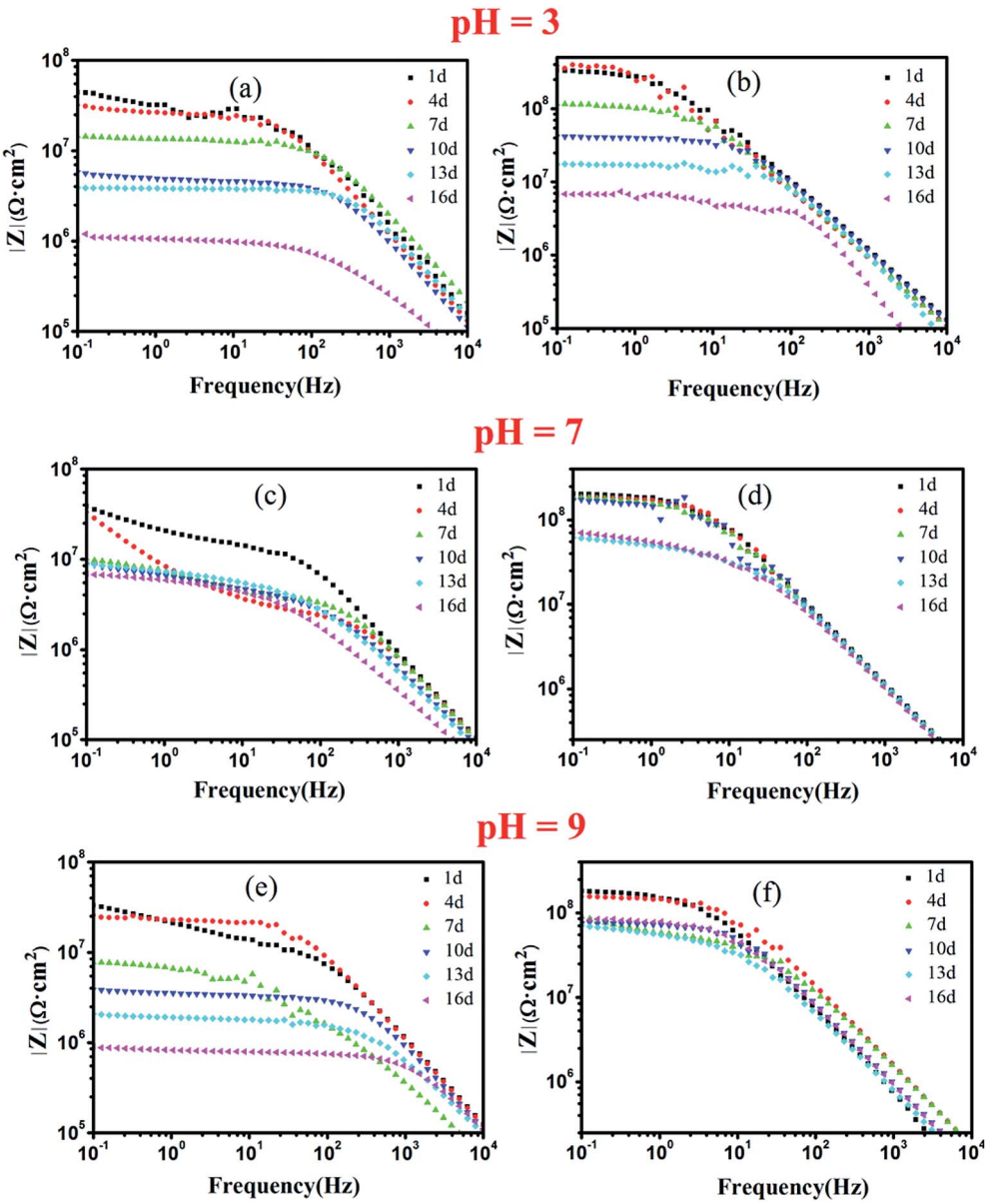

Fig. 8 Bode plots of waterborne EA coatings filled with (a) PANI; (b) c–PANI in 3.5 wt% NaCl medium of (a, b) pH 3; (c, d) pH 7; (e, f) pH 9.

corrosion protection. From the Tafel curve and Table 1, high corrosion voltages and low corrosion currents can be observed in the case of coating filled with c–PANI in acidic, neutral and alkaline conditions compared with the coating PANI. The corrosion voltage and corrosion current show slightly difference between PANI and c–PANI coatings in acidic condition, but much difference in neutral and alkaline conditions. These results indicate the better corrosion protection of the coatings with c–PANI as the filler than that of the coatings filled with PANI, which is consistently with the results of Bode curve.

To confirm the passivation effect of c–PANI on metal surface in acid medium, XPS analysis was performed on the steel surface whose coating was peeled off after soaked for 35 days. The XPS Fe 2p spectra are shown in Fig. 11. In the case of pH 7 and pH 9, two sharp peaks appeared at 706.2 eV and 719.1 eV corresponding to Fe $2p_{3/2}$ and $2p_{1/2}$ lines of metallic iron (Fe^0), respectively. Another two peaks appeared at 710.1 and 723.5 eV assignable to Fe $2p_{3/2}$ and $2p_{1/2}$ lines of trivalent iron (Fe^{3+}) in Fe_2O_3, respectively.[40] This result suggests that c–PANI with redox activity in the medium of pH 7 and pH 9 has good barrier property against corrosion medium penetrating, leading to no passivation effect detected. Differently, in the case of pH 3, two sharp peaks 711.2 eV and 724.5 eV appeared, and a new weak satellite feature emerged around 717 eV, indicating a dense oxide layer of Fe_3O_4 was formed on the steel surface, which confirm the passivation effect of c–PANI coating in acidic medium. It can be concluded that the good barrier property of c–PANI coating against neutral and alkaline corrosion medium penetrating and predominately passivation protection of c–PANI nanobrushes at acidic medium offer anti-corrosion protection for steels over a wide pH range.

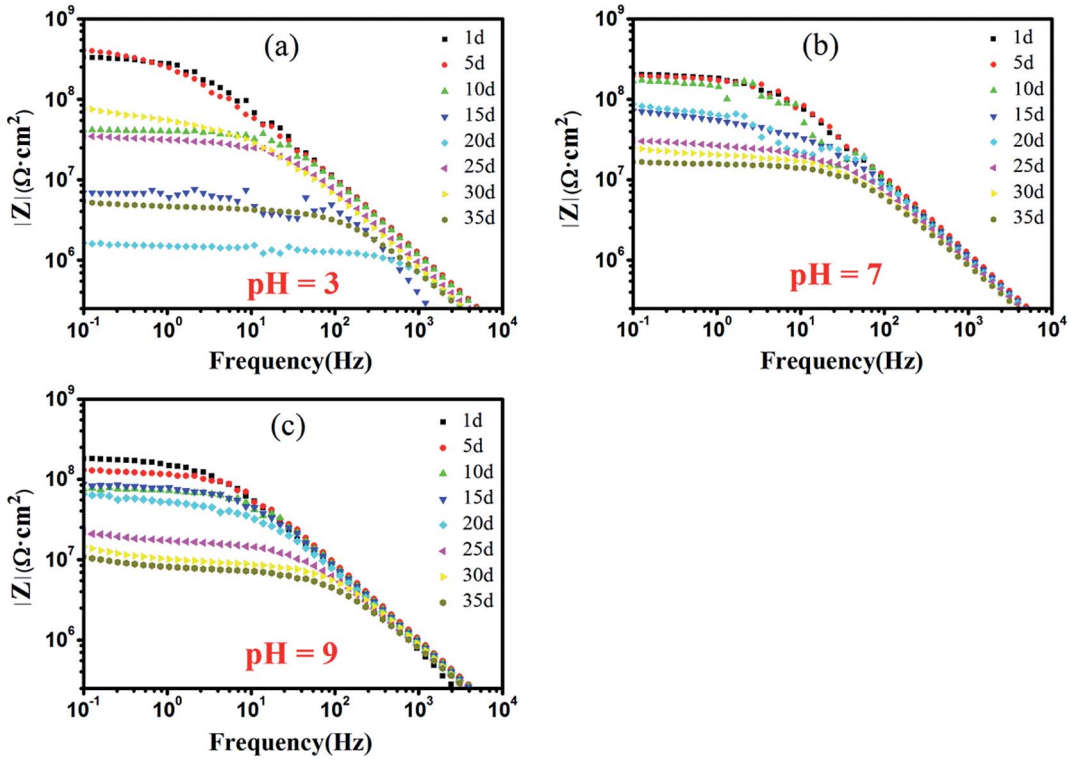

Fig. 9 Bode plots of waterborne c–PANI coating in 3.5 wt% NaCl medium of: (a) pH 3; (b) pH 7; (c) pH 9.

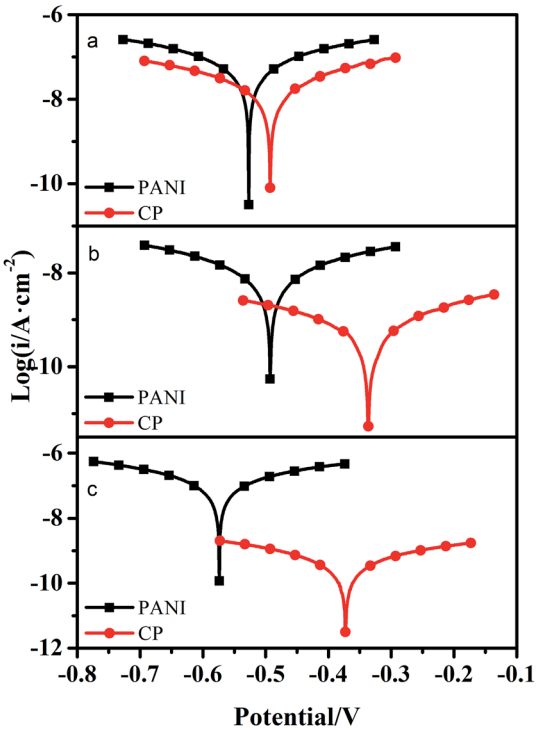

Fig. 10 Tafel plots for PANI and c–PANI coating electrodes measured in (a) pH 3; (b) pH 7; (c) pH 9 in 3.5% NaCl aqueous solution after immersion for 16 days.

Table 1 Electrochemical corrosion measurements of PANI-coated and c–PANI-coated in different solution

Coatings	E_{corr}/V	I_{corr}/A cm^{-2}
PANI (pH 3)	−0.527	6.83×10^{-8}
c–PANI (pH 3)	−0.493	2.10×10^{-8}
PANI (pH 7)	−0.493	9.40×10^{-9}
c–PANI (pH 7)	−0.336	5.87×10^{-10}
PANI (pH 9)	−0.574	1.27×10^{-7}
c–PANI (pH 9)	−0.373	4.52×10^{-10}

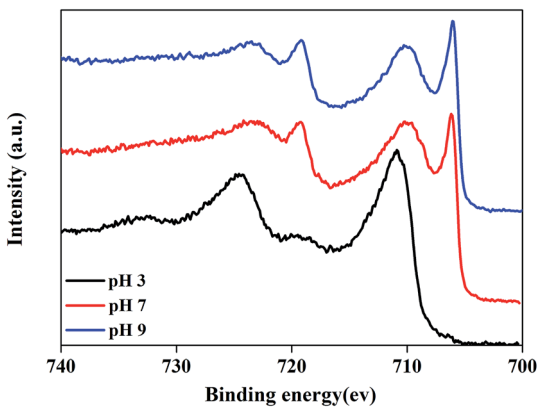

Fig. 11 XPS Fe 2p spectra of steel surface under c–PANI coating after soaked in medium of pH 3, 7 and 9 for 35 days.

4. Conclusions

The c–PANI nanobrushes with hierarchically structure have been successfully prepared by *in situ* oxidative polymerization of aniline in the presence of c-MWNTs. The thickness of PANI wrap can be tailored through varying the mass ratios of c-MWNTs to aniline. The unique brushes morphology of the composites leads to the formation of a new charge transfer bridge through π–π stacking and hydrogen bonding interactions, resulting in a higher electrochemical activity than PANI in acidic, neutral and alkaline environments. The anticorrosion mechanism of c–PANI containing waterborne EA coating presented excellent passivation protection for carbon steel in acidic solution and physical barrier in the neutral and alkaline solution. The novel carbon nanotube–polyaniline nanobrushes reported here offer a number of advantages, including low cost, easy performance, environmentally friendly, and high electroactivity over a wide pH range, opening any number of opportunities for application of anticorrosion protection of metals.

Acknowledgements

This research was financially supported by a grant from the College and University Key Project of Jiangsu Province (No. 14KJA430006), Prospective United Innovation Project of Jiangsu Province (No. SBY2014020171), Guangdong Province Science & Technology Program (No. 2017A010103015), start-up funding from South China Agricultural University (4900-216489) and Science and Technology Cooperation Funds of Yangzhou City and Yangzhou University (YZ2016250).

References

1 C. O. Baker, X. W. Huang, W. Nelson and R. B. Kaner, *Chem. Soc. Rev.*, 2017, **46**, 1510–1525.
2 Y. Zhang, M. A. Qiu, Y. Yu, B. Y. Wen and L. L. Cheng, *ACS Appl. Mater. Interfaces*, 2017, **9**, 809–818.
3 X. H. Sun, N. Zhang and X. Q. Huang, *Chemcatchem*, 2016, **8**, 3436–3440.
4 G. F. Cai, J. X. Wang and P. S. Lee, *Acc. Chem. Res.*, 2016, **49**, 1469–1476.
5 M. A. Deyab, *J. Power Sources*, 2014, **268**, 50–55.
6 B. L. He, Q. W. Tang, T. L. Liang and Q. H. Li, *J. Mater. Chem. A*, 2014, **2**, 3119–3126.
7 J. Mahmood, E. K. Lee, M. Jung, D. Shin, H. J. Choi, J. M. Seo, S. M. Jung, D. Kim, F. Li, M. S. Lah, N. Park, H. J. Shin, J. H. Oh and J. B. Baek, *Proc. Natl. Acad. Sci. U. S. A.*, 2016, **113**, 7414–7419.
8 K. Wang, Q. H. Meng, Y. J. Zhang, Z. X. Wei and M. H. Miao, *Adv. Mater.*, 2013, **25**, 1494–1498.
9 Y. Y. Yang, Y. F. Hao, J. H. Yuan, L. Niu and F. Xia, *Carbon*, 2014, **78**, 279–287.
10 D. W. DeBerry, *J. Electrochem. Soc.*, 1985, **132**, 1022–1026.
11 J. Q. Xu, Y. Q. Zhang, D. Q. Zhang, Y. M. Tang and H. Cang, *Prog. Org. Coat.*, 2015, **88**, 84–91.
12 C. W. Peng, K. C. Chang, C. J. Weng, M. C. Lai, C. H. Hsu, S. C. Hsu, Y. Y. Hsu, W. I. Hung, Y. Wei and J. M. Yeh, *Electrochim. Acta*, 2013, **95**, 192–199.
13 X. X. Sheng, W. X. Cai, L. Zhong, D. L. Xie and X. Y. Zhang, *Ind. Eng. Chem. Res.*, 2016, **55**, 8576–8585.
14 G. Williams and H. N. McMurray, *Electrochim. Acta*, 2009, **54**, 4245–4252.
15 J. Fang, K. Xu, L. H. Zhu, Z. X. Zhou and H. Q. Tang, *Corros. Sci.*, 2007, **49**, 4232–4242.
16 B. Wessling and J. Posdorfer, *Electrochim. Acta*, 1999, **44**, 2139–2147.
17 A. Talo, P. Passiniemi, O. Forsen and S. Ylasaari, *Synth. Met.*, 1997, **85**, 1333–1334.
18 Y. Chen, X. H. Wang, J. Li, J. L. Lu and F. S. Wang, *Corros. Sci.*, 2007, **49**, 3052–3063.
19 F. Chen and P. Liu, *ACS Appl. Mater. Interfaces*, 2011, **3**, 2694–2702.
20 S. L. Mu, *Synth. Met.*, 2004, **143**, 259–268.
21 S. L. Mu, *Synth. Met.*, 2011, **161**, 1306–1312.
22 S. J. Tian, A. Baba, J. Y. Liu, Z. H. Wang, W. Knoll, M. K. Park and R. Advincula, *Adv. Funct. Mater.*, 2003, **13**, 473–479.
23 E. Simon, C. M. Halliwell, C. S. Toh, A. E. G. Cass and P. N. Bartlett, *J. Electroanal. Chem.*, 2002, **538**, 253–259.
24 J. Y. Liu, S. J. Tian and W. Knoll, *Langmuir*, 2005, **21**, 5596–5599.
25 H. J. Zhou, Y. Q. Lin, P. Yu, L. Su and L. Q. Mao, *Electrochem. Commun.*, 2009, **11**, 965–968.
26 W. Feng, X. D. Bai, Y. Q. Lian, J. Liang, X. G. Wang and K. Yoshino, *Carbon*, 2003, **41**, 1551–1557.
27 E. Coskun, E. A. Zaragoza-Contreras and H. J. Salavagione, *Carbon*, 2012, **50**, 2235–2243.
28 S. Quillard, G. Louarn, S. Lefrant and A. G. Macdiarmid, *Phys. Rev. B: Condens. Matter Mater. Phys.*, 1994, **50**, 12496.
29 Q. G. Wang, X. Qian, S. M. Wang, W. Zhou, H. Guo, X. M. Wu, J. P. Li and X. H. Wang, *Synth. Met.*, 2015, **199**, 1–7.
30 X. S. Zhou, T. B. Wu, B. J. Hu, G. Y. Yang and B. X. Han, *Chem. Commun.*, 2010, **46**, 3663–3665.
31 T. M. Wu and Y. W. Lin, *Polymer*, 2006, **47**, 3576–3582.
32 P. Kar and A. Choudhury, *Sens. Actuators, B*, 2013, **183**, 25–33.
33 Q. Yao, L. D. Chen, W. Q. Zhang, S. C. Liufu and X. H. Chen, *ACS Nano*, 2010, **4**, 2445–2451.
34 L. V. Lukachova, E. A. Shkerin, E. A. Puganova, E. E. Karyakina, S. G. Kiseleva, A. V. Orlov, G. P. Karpacheva and A. A. Karyakin, *J. Electroanal. Chem.*, 2003, **544**, 59–63.
35 M. A. Bavio, G. G. Acosta and T. Kessler, *J. Power Sources*, 2014, **245**, 475–481.
36 Y. Zhou, Z. Y. Qin, L. Li, Y. Zhang, Y. L. Wei, L. F. Wang and M. F. Zhu, *Electrochim. Acta*, 2010, **55**, 3904–3908.
37 J. Zhang, L. B. Kong, B. Wang, Y. C. Luo and L. Kang, *Synth. Met.*, 2009, **159**, 260–266.
38 X. G. Li, H. Y. Wang and M. R. Huang, *Macromolecules*, 2007, **40**, 1489–1496.
39 A. Adhikari, P. Claesson, J. Pani, C. Leygraf, A. Deidinaitei and E. Blomberg, *Electrochim. Acta*, 2008, **53**, 4239–4247.
40 T. Yamashita and P. Hayes, *Appl. Surf. Sci.*, 2008, **254**, 2441–2449.